Stabilization of Quantum Energy Flows within the Approximate Quantum Trajectory Approach†

Sophya Garashchuk* and Vitaly Rassolov

Department of Chemistry and Biochemistry, University of South Carolina, Columbia, South Carolina 29208

Received: March 30, 2007; In Final Form: June 20, 2007

The hydrodynamic, or the de Broglie−Bohm, formulation provides an alternative to the conventional time-dependent Schrödinger equation based on quantum trajectories. The trajectory dynamics scales favorably with the system size, but it is, generally, unstable due to singularities in the exact quantum potential. The approximate quantum potential based on the fitting of the nonclassical component of the momentum operator in terms of a small basis is numerically stable but can lead to inaccurate large net forces in bound systems. We propose to compensate errors in the approximate quantum potential by applying a semiempirical friction-like force. This significantly improves the description of zero-point energy in bound systems. Examples are given for one-dimensional models relevant to nuclear dynamics.

I. Introduction

The hydrodynamic, or the de Broglie−Bohm,[1] formulation of the time-dependent Schrödinger equation (SE) is a conceptually appealing alternative to the conventional SE. It is based on the wavefunction written in terms of real amplitude $A(x, t)$ and phase $S(x, t)$ (eq 1).

$$\psi(x, t) = A(x, t) \exp\left(\frac{i}{\hbar} S(x, t)\right) \tag{1}$$

After substitution of eq 1 into the SE for a particle of mass m and identification of the gradient of the phase with the trajectory momentum given by eq 2,

$$\nabla S(x, t) = p(x, t) \tag{2}$$

$\psi(x, t)$ can be represented in terms of trajectories characterized by positions $x(t)$ and momenta $p(t)$ evolving according to Newton's equation of motion under the combined influence of the external potential V and the quantum potential U defined below (eq 3),

$$\frac{dx(t)}{dt} = \frac{p(t)}{m} \quad \frac{dp(t)}{dt} = -\nabla(V + U) \tag{3}$$

The action function defining the wavefunction phase evolves as eq 4.

$$\frac{dS[x(t)]}{dt} = \frac{p^2}{2m} - V - U \tag{4}$$

Evolution of the probability density $\rho(x, t) = A^2(x, t)$ along these trajectories satisfies the continuity equation (eq 5),

$$\frac{d\rho(x, t)}{dt} = -\frac{\nabla p}{m}\rho(x, t) \tag{5}$$

but we prefer to work with the probability (eq 6),

$$w[x(t)] = A^2(x, t)\, dx_t \tag{6}$$

where dx_t is the volume element associated with each trajectory. For time-independent V, this probability does not change in time (eq 7).[2]

$$dw[x(t)]/dt = 0 \tag{7}$$

This trajectory description can be viewed as the most local representation of quantum mechanics, because the probability associated with a particular trajectory is independent of other trajectories. An important technical consequence of this locality is that a wavefunction always remains localized on the initially chosen set of trajectories. Equations 3 and 4 are almost the same as in classical mechanics. The difference between the dynamics of classical and quantum trajectories is due to the force associated with a single nonlocal quantity: the quantum potential (eq 8).

$$U = -\frac{\hbar^2}{2m}\frac{\nabla^2 A}{A} \tag{8}$$

We will refer to the expectation value of the quantum potential $\langle U \rangle$ as the quantum energy, because the remaining contributions to the total energy of a system have classical counterparts.

The appeal of the Bohmian formulation is two-fold: (i) it provides an intuitive visualization tool for quantum dynamics and is used to interpret conventionally obtained wavefunctions,[3] and (ii) positions of quantum trajectories provide an ideally compact time-dependent grid representation of the wavefunction. This feature is highly desirable in multidimensional calculations as the cost of standard methods of solving SE based on fixed grids or direct-product basis sets scales exponentially with the dimensionality of a system. Because of the singularities in the quantum potential at the wavefunction nodes, dynamics of quantum (Bohmian) trajectories describing time-evolution of all but Gaussian wavefunctions is, generally, numerically unstable. The problem is especially severe for bound anharmonic potentials, where even slight anharmonicity results in a rapid deterioration of numerical accuracy. Several strategies dealing with this problem have been proposed over the past few years,

† Part of the special issue "Robert E. Wyatt Festschrift".

* To whom correspondence should be addressed. E-mail: sgarashc@mail.chem.sc.edu.

10.1021/jp072509n CCC: $37.00
Published on Web 08/03/2007

including mixed Lagrangian−Eulerian grids,[4] covering functions,[5] and artificial viscosity.[6]

The quantum trajectory formulation also provides a natural connection with classical mechanics. The quantum potential for nonsingular wavefunctions vanishes in the semiclassical limit of $\hbar \to 0$ or $m \to \infty$ and can serve as a starting point for semiclassical dynamics methods, including the approximate quantum potential (AQP) method pursued by this group. Other approximate methods include the derivative propagation method of Trahan and Wyatt,[7] the local quadratic expansions of Zhao and Makri,[8] and the classical/quantum correspondence of Poirier.[9]

The quantum potential (eq 8) depends only on wavefunction density, and therefore, simple AQP can be derived based on the density fit to a particular functional form, such as a Gaussian or a linear combination of Gaussians.[10] A much more elegant approach is based on the fit to the nonclassical momentum,[11]

$$r(x, t) = \frac{\nabla A(x, t)}{A(x, t)} \tag{9}$$

from which the approximate quantum force is derived. This approach has been further developed to include energy conservation,[12] optimization on subspaces,[13] arbitrary coordinate systems,[14] and nonadiabatic dynamics.[15] It has been successfully applied in reactive scattering to $H + H_2$ and to the nonadiabatic $O + H_2$ systems.[16] In these applications, an accurate description of motion in vibrational coordinates for several oscillation periods was achieved by defining AQP on subspaces or by including the exponential function (exact for the eigenstates of the Morse potential[17]) into the AQP. In condensed systems it is desirable, however, to describe vibrational motion, in particular, its zero-point energy, on a much longer, essentially arbitrarily long, time-scale in an efficient manner. One of the simplest globally defined quadratic AQPs is exact for Gaussian wavefunctions, but although numerically stable, it quickly loses accuracy in anharmonic systems. Below we introduce a semiempirical "friction", alleviating this behavior in anharmonic systems. Examples are given for one-dimensional systems analyzed in ref 13. The formalism is described in atomic units (au) in one dimension. Multidimensional generalization is given where necessary.

II. Theory

The simplest nontrivial AQP is based on the linear approximation (eq 10)

$$\tilde{r} = a(t)x + b(t) \tag{10}$$

to the nonclassical momentum r of eq 9 and gives the linearized quantum force (LQF). As described in ref 12, the expansion coefficients a and b are found from the minimization of a functional (eq 11),

$$I = \int (r - \tilde{r})^2 \rho(x, t)\, \mathrm{d}x_t \tag{11}$$

which is shown to be equivalent to maximization of the AQP (eq 12).

$$\tilde{U} = -\frac{1}{2m}(\tilde{r}^2 + \tilde{r}') \tag{12}$$

With the AQP of eq 12, the total energy of the system is conserved regardless of the quality of the approximation. This approach exactly describes an arbitrary Gaussian wavefunction evolving in a locally quadratic potential and reproduces energy spread in a wavepacket. However, in bound anharmonic systems, trajectory motion soon becomes chaotic; trajectories "decohere" and lose their quantum or, for the ground state, zero-point energy (ZPE). In the semibound potentials, such as the Morse potential, inaccuracies in the quantum force on the fringes of the wavepacket lead to some trajectories moving to the dissociation limit, which "drains" energy from the bound trajectories and reduces ZPE. For an accurate description of an eigenstate, quantum force should cancel classical force exactly; as for the Morse potential, it was achieved by using an exponential function in $\tilde{r}$.[14]

Within a simpler and more general linear approximation to r, we propose to use a semiempirical friction-like force compensating for the inaccuracies of the AQP. We impose several requirements on such a force: (i) it should be Galilei invariant and it should vanish (ii) when the propagation is exact and (iii) in the classical limit of zero quantum potential; (iv) in addition, if, in case of separable motion, there are exact and approximate degrees of freedom, this force should not influence the exact degrees of freedom.

We start by considering a Gaussian wavepacket with the corresponding linear r and p. At time t the AQP error in the anharmonic potential results in the error in trajectory momenta $\delta p(t)$ and in position (eq 13).

$$\delta x(t) = \int_0^t \frac{\delta p(\tau)}{m}\, \mathrm{d}\tau \tag{13}$$

The error in quantum force associated with $\delta x(t)$ is estimated from the expansion of the quantum potential in $\delta x(t)$ up to second-order (eq 14),

$$U[x(t) + \delta x(t)] \approx U[x(t)] + U'[x(t)] \int_0^t \frac{\delta p(\tau)}{m}\, \mathrm{d}\tau \tag{14}$$

resulting in a deviation of the force (δF) in the Newton's equation of motion (eq 15).

$$\delta F = -\frac{\mathrm{d}}{\mathrm{d}x}\left(U'[x(t)] \int_0^t \frac{\delta p(\tau)}{m}\, \mathrm{d}\tau\right) \tag{15}$$

Therefore, neglecting the unknown spatial derivative of δp, we introduce a friction-like force ($F_{\mathrm{fr}} \approx -\delta F$) to compensate for this error. In the multidimensional case this force is given by eq 16;

$$F_{\mathrm{fr}} = \eta(\nabla \cdot \nabla^T U[\vec{x}(t)]) \int_0^t \frac{\delta \vec{p}(\tau)}{m}\, \mathrm{d}\tau \tag{16}$$

where $\nabla \cdot \nabla^T U$ is the Hessian matrix of the quantum potential. In eq 16 we have introduced the friction coefficient η, which should be set to 1 if the expansion in eq 14 was exact. In practice, we treat it as an adjustable parameter. Using velocity ($v = p/m$) and the AQP of eqs 10 and 12, the friction force becomes eq 17.

$$F_{\mathrm{fr}} = -\frac{\eta a^2(t)}{m} \int_0^t (v(\tau) - \tilde{v}(\tau))\, \mathrm{d}\tau \tag{17}$$

The deviation in momenta for each trajectory $\delta p(t) = p(t) - \tilde{p}(x, t)$ is defined with respect to a global linear in position fit ($\tilde{p}(x, t)$) to the momenta $p(t)$. The parameters of the fit (different from those of $\tilde{r}$) are obtained from the standard least-square fit procedure[18] minimizing $\langle (p - \tilde{p})^2 \rangle$. The derivative of $\delta p(t)$, neglected within eq 16, is zero in this approximation. If the globally defined linear $\tilde{r}$ and $\tilde{p}$ are inaccurate, then eq 17 can be generalized to linear approximations on subspaces.[13] With

the friction force of eq 17 the equations of motion of the quantum trajectories become eq 18.

$$\frac{dx(t)}{dt} = \frac{p(t)}{m} \quad \frac{dp(t)}{dt} = -\frac{d}{dx}(V + U) + F_{fr} \qquad (18)$$

This additional force (F_{fr}) is similar to the conventional friction force due to the interaction with the environment[19] that is generally written as eq 19.

$$F = -\int_0^t \eta(t-\tau)v(\tau)\, d\tau \qquad (19)$$

Both arise from the incomplete knowledge of the system, and both depend on the time-dependent friction coefficient and on the integral of the velocity. However, the "quantum" friction of eq 17 depends on the deviation of the velocity of the quantum trajectories from the exact velocity. In the case of the linear quantum force, the exact dynamics results in a linear dependence of velocity on position.

It is easy to see that the requirements set forth above are satisfied for F_{fr} of eq 17. The time-dependent prefactor analogous to the friction coefficient goes to zero in the classical regime if the quantum force is zero. The quantum friction also vanishes if dynamics is exact (i.e., $\delta p = 0$). In the multidimensional case for a separable Hamiltonian and a factorizable initial wavefunction, the friction force is equal to zero in the exact degree of freedom labeled j, because the momentum deviation $\delta p_j(t) = 0$ and $\nabla_{ij}^2 U = 0$ for $i \neq j$ in the course of dynamics, and the motion along the approximate degree of freedom is unaffected by the exact one. An important difference with the conventional friction is that quantum friction does not necessarily decrease the energy of the system. Energy nonconservation can be used to monitor the effect of the quantum friction and to adjust the friction coefficient η.

To test the validity of the arguments leading to eq 17, let us consider the dynamics of a coherent Gaussian wavepacket (eq 20),

$$\psi(x, t) = \sqrt{\frac{2}{\pi}} \exp\Big(-(x - x_t)^2 + \imath p_t(x - x_t) + \frac{\imath}{2}(x_t p_t - x_0 p_0 - t)\Big) \qquad (20)$$

which is the solution of SE with $m = 1$ and $V = x^2/2$. Parameters x_t and p_t, $x_t = x_0 \cos t + p_0 \sin t$, and $p_t = p_0 \cos t - q_0 \sin t$, describe the motion of the center of this wavepacket. The initial momenta of all quantum trajectories are equal to p_0. We displace the initial momentum of one of the trajectories ($p(0) = p_0 + dp$) and let it evolve under the combined influence of the classical, exact quantum, and friction forces. (The weight of a single trajectory can be made vanishingly small, so that its displacement will not affect the linearity of r and p of the remaining trajectories.) Figure 1 shows the phase portraits of a trajectory with initial conditions $q(0) = 1.5$ without the displacement ($p(0) = p_0$) and with the displacement ($dp = -0.1$). The parameters of $\psi(x, 0)$ are $x_0 = 1$ and $p_0 = 1$. As seen from Figure 1a, without the friction force the displaced trajectory begins to spiral and drift away as opposed to the circular motion of the exact trajectory. Introduction of the friction force counteracts this drift and makes the trajectory oscillate around a circular path of a smaller radius because it has a smaller initial momentum, shown in Figure 1b, compared to the undisplaced trajectory. Note that $\eta = 1$ corresponds to the oscillations of the smallest amplitude, reflecting the fact that expansion in eq 14 is exact for the quadratic potential.

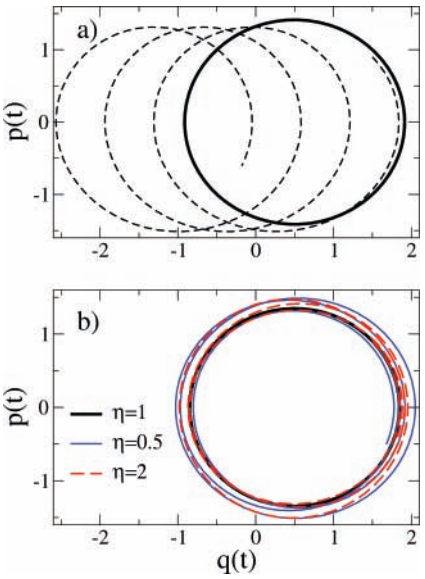

Figure 1. Displaced quantum trajectories for a coherent Gaussian wavepacket: (a) momenta vs positions of trajectories without (solid line) and with the initial displacement (dash); (b) momenta vs positions of the initially displaced trajectories with the friction force coefficient $\eta = \{1, 0.5, 2\}$.

III. Results and Discussion

In this section we analyze the effect of the friction force on dynamics with the globally defined quadratic AQP producing linear quantum force. Special attention is given to the long-time description of bound motion and time-dependence of quantum energy or ZPE. Model systems are the same as in ref 13 and are chosen for their relevance to problems of nuclear dynamics. The quantum-mechanical (QM) results used for comparison were obtained using the split-operator method.[20] The AQP results are obtained by propagating trajectories as specified by eq 18. The action function $S(x, t)$ of eq 4 and the time integral of the momentum deviation $\delta p(t)$ needed to evaluate the friction force (eq 17) are accumulated in time for each trajectory. Linear fits to the classical and nonclassical components of the momentum operator ($\tilde{r}$ and $\tilde{p}$, computed at each time step as discussed in Section II), give the approximate quantum potential and quantum force and the friction force. In the AQP calculations we typically used 399 trajectories propagated with time-increments that are 25 times smaller than the time-step of QM propagation (and 5 times smaller than propagation with the classical force) because the quantum and friction forces are time-dependent. The numerical effort of computing the friction force is negligible as compared to the AQP computation, because minimization of both r and p require inversion of the same matrix. The AQP calculations took twice as long as the QM propagation and were five times longer than the purely classical propagation, which is explained by low dimensionality of the problem and simple analytical form of the potentials considered. For realistic multidimensional problems, the cost of AQP calculation becomes a small fraction of the total computation cost.

We have verified that the friction force of eq 17 does not prevent bifurcation of the wavepacket under the influence of the external force by analyzing dynamics of the Eckart barrier described in ref 13. For this scattering problem the prefactor $a^2(t)$ in eq 17 vanishes faster than the accumulation of δp, and the effect of the friction force is negligible.

A. Perturbed Harmonic Oscillator. Our first application is dynamics of a Gaussian wavepacket in the anharmonic potential studied in ref 21. The potential is a harmonic oscillator perturbed

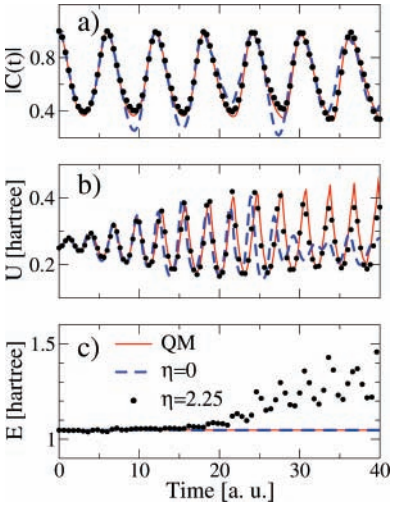

Figure 2. Dynamics in the potential with quartic anharmonicity. (a) The amplitude of the auto-correlation function, $C(t) = \langle\psi(0)|\psi(t)\rangle$, (b) quantum energy, $\langle U\rangle$, and (c) total energy of the system as a function of time are obtained with the LQF method for $\eta = 0$ (dash line), $\eta = 2.25$ (circles). The quantum result is shown with a solid line on all panels.

by a quartic potential: $V = x^2/2 + 0.01x^4$, $m = 1$. The initial wavefunction is a displaced Gaussian (eq 21),

$$\psi(x, 0) = (2\alpha/\pi)^{1/4} \exp(-\alpha(x - x_0)^2 + \imath p_0(x - x_0)) \quad (21)$$

with the values $\alpha = 0.5$, $x_0 = 1.0$, $p_0 = 0.0$. The anharmonicity is small, and the motion of the center of the wavepacket remains essentially harmonic. Nevertheless, we see that, with the LQF method, trajectories on the fringes of the wavepacket quickly "decohere" analogously to the drift of the displaced trajectory shown on Figure 1a. This leads to errors in the phase sensitive quantities, such as wavepacket correlation function ($C(t)$, shown on Figure 2a) and to the loss of quantum energy, shown on Figure 2b, after 6 oscillation periods. For a real initial wavepacket the autocorrelation function is computed by eq 22.

$$C(t) = \langle\psi(0)|\psi(t)\rangle = \sum_i w_i \exp(2\imath S(x_i, t/2)) \quad (22)$$

The total energy shown in Figure 2c is conserved within the LQF formalism. The friction force reduces this decoherence and improves agreement of $C(t)$ and, most importantly, of the quantum energy. Total energy is not conserved when the friction is introduced, but it serves as a guide for choosing a value of η. For quadratic potentials the value of η is one, but we find that it should be adjusted in the presence of anharmonicity. For the given system, $\eta = 1$ leads to an unstable regime as total energy of the system increases. However, larger values of η improve the performance of the LQF method. The value $\eta = 2.25$ giving stable dynamics was used in this calculation. We find that further increase of the friction coefficient (up to $\eta = 10-20$) suppresses chaotic motion of the trajectories for up to 100 oscillation periods. This regime, which gives accurate results for the perturbed harmonic oscillator, is very different from the derived value of $\eta = 1$ and could qualitatively change the dynamics in general systems by preventing bifurcations. Therefore, we choose the smallest η, yielding total energy oscillating within a few percent around its initial value.

B. Morse Oscillator. Next, we consider the ground state of the Morse oscillator. The purpose is to assess how the AQP with friction describes the ZPE of a chemical bond. The potential V describes a non-rotating H_2 molecule, $V = D(1 - \exp(-z(x - x_e))^2$. With $m = 1.15$, the parameters of the potential in scaled atomic units are $D = 160.0$, $x_e = 1.4008$, and $z = 1.0435$. We apply the quantum trajectory formalism to the propagation of the ground state $\psi(x, 0)$ and examine the density overlap ($C(t) = \langle\rho(0)|\rho(t)\rangle$), quantum energy, and total energy. Figure 3 shows the three quantities on panels a−c, respectively. The main deficiency of the global linearization of the quantum force is that it does not compensate for the external force exactly (as it should for the ground state). Consequently, trajectories on the fringes of the wavepacket experience large inaccurate forces that push them into the dissociation region of the potential, reducing the energy of the remaining bound trajectories. This effect can be seen in the behavior of the quantum energy on panel b and in the time-dependence of $C(t)$. Introduction of friction force with $\eta = 1$ decreases the number of dissociating trajectories but does not eliminate this behavior completely. From the time-dependence of the total energy on Figure 3c we see that this friction drains a considerable amount of energy from the system. A larger value of η ($\eta = 2.5$) produces stable dynamics with a small loss of quantum and total energies.

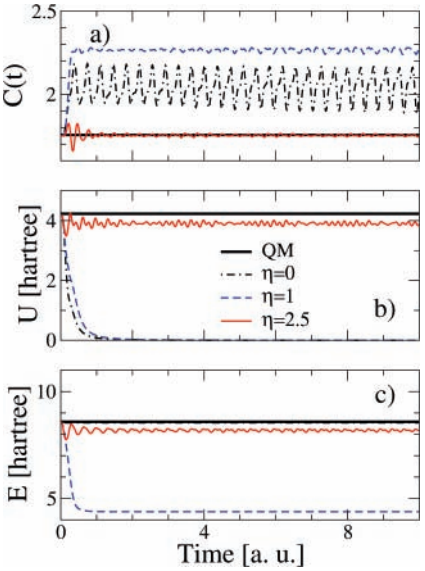

Figure 3. Dynamics in the Morse potential. (a) The amplitude of the density correlation function, $C(t) = \langle\rho(0)|\rho(t)\rangle$, (b) quantum energy, $\langle U\rangle$, and (c) total energy of the system as a function of time are obtained with the LQF method for $\eta = 0$ (dot-dash line), $\eta = 1$ (dash line) and $\eta = 2.5$ (thin solid line). The quantum result is shown with a thick solid line on all panels. On panel c) the result for $\eta = 0$ is indistinguishable from the exact energy.

Consistent with the derivation, the value of the adjustable parameter η depends upon the anharmonicity of the system. Results given in Table 1 support this claim. We examined which smallest η gives stable dynamics of the Morse oscillator eigenstate for several isotopes (including fictitious heavy nuclei). Dynamics of heavier isotopes is stabilized by smaller values of η. The resulting ZPE is less oscillatory and is in better agreement with the exact result. We also looked at the ZPE of a Gaussian wavepacket mimicking the ground state and displaced by ± 0.1 from the bottom of the well and observed the same trend. The stabilizing value of η increased up to 3.0/3.5 in these cases due to appreciable anharmonicity of the hydrogen molecule bond.

C. Metastable Potential Well. Finally, we consider a metastable well studied in ref 22. This system exhibits a combined bound/unbound motion. Our goal here is to test wavepacket bifurcation in the presence of a friction force. The external potential in scaled units with $m = 1$ is $V = Z(x^2 - x^3)$, where $Z = 200$. V forms a well, supporting two metastable

TABLE 1: Dependence of the Friction Coefficient (η) Resulting in Stable Dynamics on the Mass (m) for the Morse Oscillator[a]

m/m_H	η	E_0	ΔE	σ_E	U_0	ΔU	σ_U
1	2.5	8.59	0.41	0.093	4.24	0.35	0.090
2	2.3	6.10	0.22	0.032	3.02	0.19	0.038
3	2.2	4.99	0.15	0.022	2.47	0.13	0.029
5	2.1	3.87	0.09	0.014	1.92	0.08	0.020
10	2.0	2.74	0.05	0.007	1.37	0.05	0.007
20	1.8	1.94	0.02	0.004	0.968	0.023	0.006

[a] E_0 is the analytic ZPE, and U_0 is the quantum energy of the eigenstates. The terms ΔE and ΔU are the differences between the exact and AQP values, $\Delta E = E_0 - E_{AQP}$, and $\Delta U = U_0 - U_{AQP}$ averaged over 13 oscillation periods. The terms σ_E and σ_U are the standard deviations of E_{AQP} and U_{AQP}, respectively.

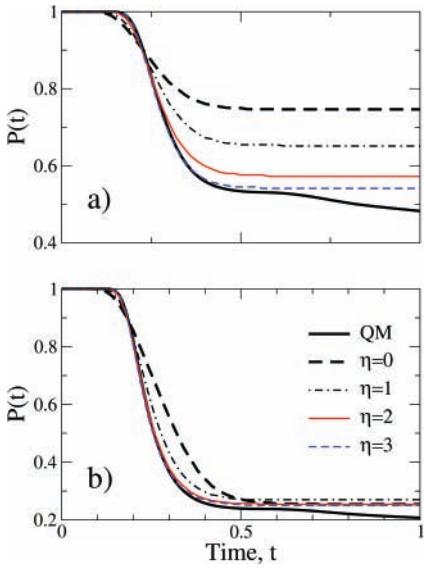

Figure 4. Survival probability in the metastable potential well for (a) $E = V^\dagger$ and for (b) $E = 2V^\dagger$. Results for values of $\eta = \{0, 1, 2, 3\}$ are compared to the quantum mechanical probability. The legend applies to both panels.

states. The energy of the barrier top, located at $x^\dagger = 0.667$, is $V^\dagger = 29.619$. Potential of the unbound region is set to a constant: $V = -V^\dagger$ for $x > 1.1184$. We examine the time-evolution of two wavepackets, defined by eq 21 and initially centered on the repulsive wall, with total energies $E_{tot} = 2V^\dagger$ and $E_{tot} = V^\dagger$. The parameters of $\psi(x, 0)$ are $\alpha = 10.0$, $p_0 = 0.0$ with $q_0 = -0.4125$ and $q_0 = -0.2821$ for the two values of E_{tot}.

Figure 4 shows the amount of the wavefunction density in the metastable well, which is the survival probability ($P(t) = \sum_{x_i(t)<x^\dagger} w_i$) for the two values of initial energy. We apply a globally linearized quantum force. Therefore, once the wavepacket bifurcates into bound and unbound components, the quantum force and the friction vanish. Such quantum force cannot reproduce the ZPE of the bound part of the wavepacket, and the exponential decay of $P(t)$ exhibited $t > 0.5$. As seen from the figure, friction force does not prevent the wavepacket from bifurcation, and $\eta > 1$ improves agreement with quantum results at short times. Accuracy of $P(t)$ correlates with the level of energy conservation.

IV. Conclusions

Ideal quantum trajectory dynamics leads to a smooth flow of noncrossing trajectories; deviations in position of trajectories produce local features in the quantum potential that restore smooth stable dynamics. To describe this response to deviation, quantum potential should be sensitive to each trajectory. Our AQP is defined globally and therefore cannot compensate for local deviations. As a compensation for this deficiency we have introduced a semiempirical friction-like force improving the description of ZPE in bound systems in the framework of quantum trajectory dynamics with the approximate quantum potential. This expands applicability of this approach to long-time dynamics of systems with bound reaction degrees of freedom, although more research is needed to make it truly general.

The functional form of the friction force is derived as the leading correction term and therefore is expected to work only for systems close to harmonic. We used this force in dynamics of wavefunctions that significantly deviate from being Gaussian, yet the general functional form of the friction force worked with the adjusted coefficient η. In addition, it might be possible to adjust values of η and/or the linear approximation of p to have a rigorous energy-conserving method. Current research on these two issues will bring us closer to our ultimate goal of developing a computationally cheap method that accounts for quantum corrections for arbitrary long propagation time in large semiclassical systems.

Acknowledgment. The authors are grateful to Bob Wyatt and Brian Kendrick for motivational discussions. This material is based upon work supported by the National Science Foundation under Grant No. CHE-0516889 and by MDA under Cooperative Agreement HQ0006-05-2-0001. The content of the information does not necessarily reflect the position or the policy of the U.S. Government, and no official endorsement should be inferred.

References and Notes

(1) Bohm, D. *Phys. Rev.* **1952**, *85*, 166−193.
(2) Garashchuk, S.; Rassolov, V. A. *J. Chem. Phys.* **2003**, *118*, 2482−2490.
(3) Sanz, A. S.; Borondo, F.; Miret-Artes, S. *J. Phys.* **2002**, *14*, 6109−6145.
(4) Trahan, C. J.; Wyatt, R. E. *J. Chem. Phys.* **2003**, *118*, 4784−4790.
(5) Babyuk, D.; Wyatt, R. E. *J. Chem. Phys.* **2004**, *121*, 9230−9238.
(6) Pauler, D. K.; Kendrick, B. K. *J. Chem. Phys.* **2004**, *120*, 603−611.
(7) Trahan, C. J.; Hughes, K.; Wyatt, R. E. *J. Chem. Phys.* **2003**, *118*, 9911−9914.
(8) Zhao, Y.; Makri, N. *J. Chem. Phys.* **2003**, *119*, 60−67.
(9) Poirier, B. *J. Chem. Phys.* **2004**, *121*, 4501−4515.
(10) Garashchuk, S.; Rassolov, V. A. *Chem. Phys. Lett.* **2002**, *364*, 562−567.
(11) Garashchuk, S.; Rassolov, V. A. *Chem. Phys. Lett.* **2003**, *376*, 358−363.
(12) Garashchuk, S.; Rassolov, V. A. *J. Chem. Phys.* **2004**, *120*, 1181−1190.
(13) Rassolov, V. A.; Garashchuk, S. *J. Chem. Phys.* **2004**, *120*, 6815−6825.
(14) Rassolov, V. A.; Garashchuk, S.; Schatz, G. C. *J. Phys. Chem. A* **2006**, *110*, 5530−5536.
(15) Garashchuk, S.; Rassolov, V. A.; Schatz, G. C. *J. Chem. Phys.* **2005**, *123*, 174108.
(16) Garashchuk, S.; Rassolov, V. A.; Schatz, G. C. *J. Chem. Phys.* **2006**, *124*, 244307.
(17) Morse, P. M. *Phys. Rev.* **1929**, *34*, 57−65.
(18) Press, W.; Flannery, B.; Teukolsky, S.; Vetterling, W. *Numerical Recipes: the Art of Scientific Computing*, 2nd ed.; Cambridge University Press: Cambridge, 1992.
(19) Caldeira, A. O.; Leggett, A. J. *Physica A* **1983**, *121*, 587.
(20) Feit, M. D.; Fleck, J. A.; Steiger, A. *J. Comput. Phys.* **1982**, *47*, 412.
(21) . Bittner, E. R. *J. Chem. Phys.* **2003**, *119*, 1358−1364.
(22) Donoso, A.; Martens, C. C. *Phys. Rev. Lett.* **2001**, *87*, 223202.